LOCAL STABILITY PERFORMANCE ANALYSIS OF ISLANDED MICROGRID BASED ON INNER CONTROL LOOPS APPROACH

Guy WANLONGO NDIWULU
Université catholique de Louvain (UCL)
Belgium
guy.wanlongo@uclouvain.be

Emmanuel DE JAEGER
Université catholique de Louvain (UCL)
Belgium
emmanuel.dejaeger@uclouvain.be

Angelo KUTI LUSALA
Université Kongo (UK)
Democratic Republic of Congo
kutilusala@gmail.com

ABSTRACT

High dynamical behavior and performance are required to maintain stable islanded microgrid operation based on inverters. However, this is strongly conditioned by the implemented control strategy as well as the characteristic parameters of the islanded microgrids. This paper investigates the influence of the controller characteristics and the microgrid parameters, on the small-signal stability of islanded microgrid. It makes the coupling between both factors in order to carry out the local stability model depending on the microgrid parameters. The islanded microgrid fed by a single inverter-based source whose control is based on inner control loops approach, is considered. The influence of each parameter is examined by analyzing the dynamical behavior of the eigenvalues in the complex plane, and the dynamical performance of the controller, with Matlab/Simulink. Accordingly, the modelling and simulation results obtained, showed that the effects of these parameters help identify and define the limits of local stability of islanded microgrids.

INTRODUCTION

Islanded microgrids are low-voltage three-phase or single-phase systems operating in remote areas. They are composed of single or hybrid micro-sources, energy storage devices, loads and control system. However, the instability of the system operation is the main issue of inverter-based islanded microgrids [1]. This is influenced by small microgrid inertia, intermittent behaviour of micro-sources, load characteristics, and microgrid parameters such as controller's gains, filters characteristics and power distribution line parameters. Among the solutions proposed in the literature, the energy storage devices are often used to reduce instabilities generated by the micro-sources [2], and the control strategies are used to solve the problems caused by the interface converters and load variations [3-4]. Nevertheless, the effects of the microgrid parameters are little investigated. The impacts of these factors cannot be neglected on the dynamical behavior and performance of islanded microgrids.

This issue requires establishing a small-signal stability model of microgrid depending on its parameters. However, the state of the art shows that the investigation on the influence of islanded microgrid parameters is mostly related to the effect of the controller parameters such as droop coefficients [5-6]. In [5], the small-signal models of the inverter, network and loads are determined using an analytical approach. Regarding the control of the inverter, this one is based on droop control. Only the influence of droop coefficients is discussed. Reference [6] investigates the effect of inverter-based sources on the small-signal stability of microgrid containing synchronous machines. The same droop control algorithm as in [5] is used. However, only the effects of droop gains are considered.

This paper proposes the study of the effects of line parameters, filter characteristics and the controller factors, on the local stability performance. This investigation is based on the dynamical model of the microgrid build from the analytical method. Compared to [5] and [6], the proposed approach uses the inner control loops approach as the control strategy implemented into the inverters. In addition, the controller factors are coupled to the filter and line parameters in order to carry out a small-signal stability model of the entire microgrid, therefore making effective the dependence between the micro-sources complexities and microgrid parameters. Finally, the effects of each parameter are assessed from the dynamical behavior of the eigenvalues in the complex plane.

The microgrid small-signal model is developed in the synchronous reference frame, and applied to the islanded microgrid fed by a single inverter-based micro-source whose control is based on the regulation of the amplitude and frequency of the voltage (V-f mode).

The remainder of the paper is organized as follows: Section II presents small-signal stability model developed for the islanded microgrid fed by a single inverter. This, in turn encompasses V-f controller model, output filter and coupling inductance, line and load model. Section III compares the performance between the proposed approach and the approach developed in [5]. Besides, it deals with the influence of the microgrid parameters on the dynamical behavior and performance of the islanded microgrid. Finally, section IV gives some conclusion including future research steps.

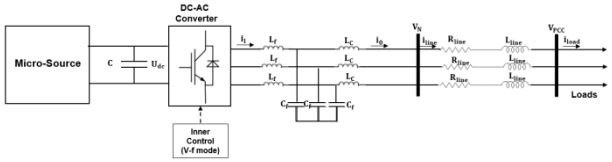

Figure 1 Islanded microgrid architecture

PROPOSED APPROACH

Islanded microgrid architecture

Figure 1 depicts the configuration of the investigated islanded microgrid. A single inverter based on inner control loops approach characterizes it. It feeds constant

impedance loads via one power distribution line, LC filter and coupling inductance L_c. This paper assumes a balanced three-phase system and three-phase voltage inverter with constant DC input voltage.

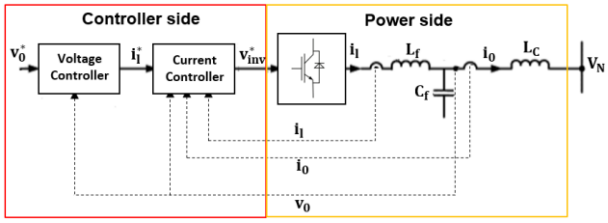

Figure 2 Block diagram of the inverter-based source

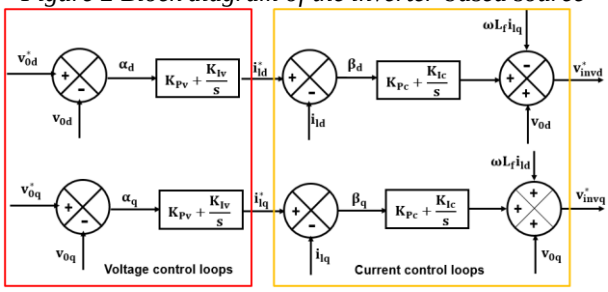

Figure 3 Algorithm of the inner control loops approach based on the V-f control mode

Small-signal stability modelling

Controller dynamical model

Figure 2 depicts the proposed approach of the inverter-based micro-source. It is characterized by the inner control loops approach in the V-f control mode. This controller is composed of external voltage control loops and internal current control loops. The first one regulates the output voltage of the filter (v_{0dq}). The voltage set-points in the d- and q-axis are settled at 320V and 0V, respectively while the internal loops controls the currents on the filter inductance L_f (i_{ldq}). Their current set-points in d-q axis are supplied by the external loops.

The controller algorithm in the synchronous reference frame is presented in Figure 3. Each control loop is characterized by a proportional and integral (PI) corrector. The feedforward voltages (v_{0dq}) and decoupling terms ($\pm\omega L_f i_{ldq}$) are added at the output of the current controller.

The linearized state-space equations of voltage and current control loops, are given by:

$$[\Delta\dot{\alpha}_{dq}] = [0][\Delta\alpha_{dq}] + A_{v1}[\Delta v^*_{0dq}] + A_{v2}\begin{bmatrix}\Delta i_{ldq}\\ \Delta v_{0dq}\\ \Delta i_{0dq}\end{bmatrix} \quad (1)$$

$$[\Delta i^*_{ldq}] = C_v[\Delta\alpha_{dq}] + E_{v1}[\Delta v^*_{0dq}] + E_{v2}\begin{bmatrix}\Delta i_{ldq}\\ \Delta v_{0dq}\\ \Delta i_{0dq}\end{bmatrix} \quad (2)$$

$$[\Delta\dot{\beta}_{dq}] = [0][\Delta\beta_{dq}] + F_{c1}[\Delta i^*_{ldq}] + F_{c2}\begin{bmatrix}\Delta i_{ldq}\\ \Delta v_{0dq}\\ \Delta i_{0dq}\end{bmatrix} \quad (3)$$

$$[\Delta v^*_{idq}] = C_c[\Delta\beta_{dq}] + G_{c1}[\Delta i^*_{ldq}] + G_{c2}\begin{bmatrix}\Delta i_{ldq}\\ \Delta v_{0dq}\\ \Delta i_{0dq}\end{bmatrix} \quad (4)$$

$$A_{v1} = \begin{bmatrix}1 & 0\\ 0 & 1\end{bmatrix} \quad A_{v2} = \begin{bmatrix}0 & 0 & -1 & 0 & 0 & 0\\ 0 & 0 & 0 & -1 & 0 & 0\end{bmatrix} \quad C_v = \begin{bmatrix}K_{Iv} & 0\\ 0 & K_{Iv}\end{bmatrix}$$

$$E_{v2} = \begin{bmatrix}0 & 0 & -K_{Pv} & 0 & 0 & 0\\ 0 & 0 & 0 & -K_{Pv} & 0 & 0\end{bmatrix} \quad E_{v1} = \begin{bmatrix}K_{Pv} & 0\\ 0 & K_{Pv}\end{bmatrix}$$

$$F_{c1} = \begin{bmatrix}1 & 0\\ 0 & 1\end{bmatrix} \quad F_{c2} = \begin{bmatrix}-1 & 0 & 0 & 0 & 0 & 0\\ 0 & -1 & 0 & 0 & 0 & 0\end{bmatrix} \quad C_C = \begin{bmatrix}K_{Ic} & 0\\ 0 & K_{Ic}\end{bmatrix}$$

$$G_{c1} = \begin{bmatrix}K_{Pc} & 0\\ 0 & K_{Pc}\end{bmatrix} \quad G_{c2} = \begin{bmatrix}-K_{Pc} & -\omega L_f & 1 & 0 & 0 & 0\\ \omega L_f & -K_{Pc} & 0 & 1 & 0 & 0\end{bmatrix}$$

Where, α_d and α_q are the direct and quadrature components of the output signal of the voltage comparator. i^*_{ld} and i^*_{lq} are the direct and quadrature components of the reference current on the filter inductance. β_d and β_q are the direct and quadrature components of output signal of the current comparator. v^*_{invd} and v^*_{invq} are the direct and quadrature components of the reference voltage at the inverter output. K_{Pv} and K_{Iv} are respectively the proportional and integral gain of the voltage control loops. K_{Pc} and K_{Ic} are the proportional and integral gain of the current control loops. v^*_{0d} and v^*_{0q} are the direct and quadrature components of the reference voltage at the filter output. And i_{od} and i_{oq} are the both components of output current of the LC filter.

PIs controllers' gains

The controllers' gains are designed through an analytical method. This in order to carry out the coupling between the gains and the microgrid parameters, such as LC filter factors and line parameters. They are given below.

$$K_{Pv} = 2\zeta\omega_{nEx}C_f \quad \text{and} \quad K_{Iv} = C_f\omega^2_{nEx} \quad (5)$$

$$K_{Pc} = 2\zeta\omega_{nIn}L - R \quad \text{and} \quad K_{Ic} = L\omega^2_{nIn} \quad (6)$$

Where, ζ is the damping factor. ω_{nEx} and ω_{nIn} are the natural frequencies of the external and internal control loops. R and L are the total resistor and inductor between the inverter output and its connection bus at the microgrid.

These expressions show that the controllers' gains are depending on the filter and line parameters. This involves that the small-signal model of the inverter depends on them too. This is illustrated in Figure 5.

Output LC filter and coupling inductance

The small-signal model of the power side is the same than that proposed in [5] and [6].

Complete model of the inverter

The small-signal models of voltage and current controllers, and output LC filter and coupling inductance constitute the global model. This one is obtained in the in D- and Q-axis common reference frame, which characterizes the microgrid. The output current of the inverter (i_{0dq}) injected to the microgrid is transformed in the D-Q reference frame. While the input voltage (v_{NDQ}) of the controller is transformed in the d-q reference frame of the controller. (7) gives the changing of reference frame for both variables (7) [5]. Where, T_S is the transformation matrix.

$$[\Delta i_{0DQ}] = [T_S][\Delta i_{0dq}] \text{ and } [\Delta v_{Ndq}] = [T_S^{-1}][\Delta v_{NDQ}] \quad (7)$$

The complete model is given by equations (8).

$$[\Delta\dot{x}_{inv}] = A_{inv}[\Delta x_{inv}] + B_{inv}[\Delta v_{NDQ}] \text{ and } [\Delta i_{0DQ}] = C_{inv}[\Delta x_{inv}] \quad (8)$$

Where, $[\Delta x_{inv}] = \left[\Delta\alpha_{dq}\ \Delta\beta_{dq}\ \Delta i_{ldq}\ \Delta v_{0dq}\ \Delta i_{0dq}\right]^T$

$$A_{inv} = \begin{bmatrix} 0 & 0 & A_{v2} \\ F_{c1}C_v & 0 & F_{c1}E_{v2} + F_{c2} \\ B_{LCl1}G_{c1}C_v & B_{LCl1}C_C & A_{LCl} + B_{LCl1}(G_{c1}E_{v2} + G_{c2}) \end{bmatrix}_{10x10}$$

$$B_{inv} = [0\ 0\ B_{LCl2}T_S^{-1}]^T_{10x2} \text{ and } C_{inv} = [0\ 0\ 0\ 0\ T_S]^T_{10x2}$$

Dynamical model of the line and load

Assuming the RL loads and that the line current (i_{line}) is the same than the load current (i_{load}) according to the microgrid architecture proposed in Figure 1. The small-signal model of the network and RL load is given by:

$$[\Delta \dot{i}_{loadDQ}] = A_{LL}[\Delta i_{loadDQ}] + B_{LL}[\Delta v_{NDQ}] \quad (9)$$

$$A_{LL} = \begin{bmatrix} 0.5(\frac{-R_{line}}{L_{line}} - \frac{R_{load}}{L_{load}}) & \omega \\ -\omega & 0.5(\frac{-R_{line}}{L_{line}} - \frac{R_{load}}{L_{load}}) \end{bmatrix}; B_{LL} = \begin{bmatrix} \frac{0.5}{L_{load}} & 0 \\ 0 & \frac{0.5}{L_{load}} \end{bmatrix}$$

Where, R_{line} and L_{line} are the resistor and inductor of the line. R_{load} and L_{load} are the resistor and inductor of loads.

Small-signal model of islanded microgrid

The complete dynamic model is given by (10). It is obtained from the dynamical sub models of the inverter, the line and the load. A virtual resistor r_N is assumed between common coupling point (PCC) bus and ground. This in order to ensure that the bus voltage is strongly defined [5]. It is taken account in the global model by using the diagonal matrix of virtual resistor R_N.

$$\begin{bmatrix} \Delta \dot{x}_{inv} \\ \Delta \dot{i}_{loadDQ} \end{bmatrix} = A\begin{bmatrix} \Delta x_{inv} \\ \Delta i_{loadDQ} \end{bmatrix} + B[\Delta v_{NDQ}]\ ;\ \begin{bmatrix} \Delta i_{0DQ} \\ \Delta v_{NDQ} \end{bmatrix} = C\begin{bmatrix} \Delta x_{inv} \\ \Delta i_{loadDQ} \end{bmatrix} \quad (10)$$

$$\text{With, } A = \begin{bmatrix} A_{inv} & 0 \\ 0 & A_{LL} \end{bmatrix}_{12x12}\ B = \begin{bmatrix} B_{inv} \\ B_{LL} \end{bmatrix}_{12x2}\ C = \begin{bmatrix} C_{inv} & 0 \\ 0 & R_N \end{bmatrix}_{4x12}$$

The factor A is the dynamical matrix of the microgrid presented in Figure 1, and (11) gives it. It is characterized by controller's gains, LC filter characteristics, and line and load parameters. The analysis of the eigenvalues of matrix A will provide information on the stability performance of the system. Among others, the influence of the characteristic parameters on these eigenvalues can be quantified. R_f , C_f and L_f are the resistor, capacitor and inductor of the LC filter. R_C and L_C are the resistor and inductor coupling the inverter to the microgrid.

$$A = \begin{bmatrix} 0 & 0 & A_{v2} & 0 \\ F_{c1}C_v & 0 & F_{c1}E_{v2} + F_{c2} & 0 \\ B_{LCl1}G_{c1}C_v & B_{LCl1}C_C & A_{LCl} + B_{LCl1}(G_{c1}E_{v2} + G_{c2}) & 0 \\ 0 & 0 & 0 & A_{LL} \end{bmatrix} \quad (11)$$

SIMULATION RESULTS

The influence of LC filter characteristics and R/X ratio of the line are investigated from the complete dynamic model with Matlab/Simulink®. Table I gives the steady-state conditions of islanded microgrid parameters.

The performance of the inverter-based model proposed is firstly compared to the model proposed in [5] from the modelling results. This is depicted in Figure 4 in which the modes of the dynamical model based on the proposed approach are in red and approach [5] in blue. It indicates that the modes are localized in the left complex plane and four groups can be observed. The first one is characterized by higher natural pulsation with the red approach compared to the blue one. It corresponds to the voltage and current controllers' modes. The second group presents the opposite effects. Then, the third group is typified by the eigenvalues introduced by the power controller in the [5] approach. Finally, the fourth group presents the same eigenvalue characteristics for the both approaches. In conclusion, similar performances can be observed between both approaches. This is the consequence of a compensation effect which can be observed between groups 1 and 2 of modes.

Figure 5 illustrates the influence of inductor and capacitor of the filter on the dynamic inverter model. For a cut-off frequency (f_{sw}) 500Hz, the results show that these factors have high impact on all complex eigenvalues. This because the inverter model depends on the both parameters. These impacts are also confirmed by the response characteristics given in Figure 6 where the oscillatory and damping frequency change with the filter characteristic variations. In addition, regarding these results, the modes 5, 6, 7 and 8 correspond to v_{0dq} and α_{dq}; 1, 2, 3 and 4 to i_{ldq} and β_{dq}; and 9 and 10 to i_{0dq}.

The microgrid dynamic model results are given in Figures 7 and 9, in which two additional complex conjugate modes 11 and 12 are observed. These are caused by both components of the current on the line i_{linedq}. Figure 7 shows the impact of the R/X ratio on the dynamical behaviour. It affects the modes 11 and 12, by moving them in the stable complex plane when this ratio decreases. Its response characteristics is illustrated in Figure 8. Where there are proved that the dynamical behaviour of the system is small affected. Then, Figure 9 gives the effects of the filter parameters on the microgrid dynamic model. It proves that only the inverter modes are impacted. In conclusion, the dynamical behaviour and performance of the system is strongly dependent on the filter characteristics according to the results obtained in Figures 6, 7, 8 and 9.

Furthermore, Figure 10 shows that the V-f controller maintains strongly the components of the voltage at their reference values.

Table I Parameters values of the system components

Line	LC Filter	RL load	Controller
Resistance(Ω/km)	Inductor	400V	ω_{nIn}
[8,41; 0,09]	[5mH; 30mH]	25kW	400 (rad/s)
Reactance(Ω/km)	Capacitor	0.25kVar	ω_{nEx}
[1,41; 0,17]	[200µF; 4µF]	v_{0d}^*	4000(rad/s)
	Resistor	320V	Damping
	$R_f = 0.5\Omega$	v_{0q}^*	$\zeta = 0,8$
	$f_{sw} = 500Hz$	0	f = 50Hz

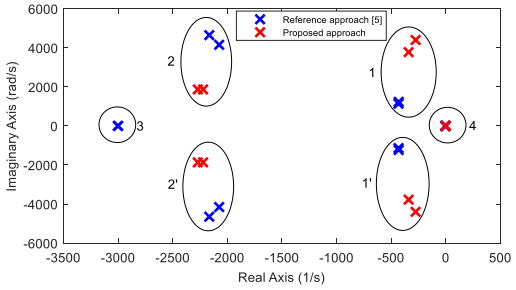

Figure 4 Eigenvalues of the dynamic inverter model based on the proposed approach and approach [5]

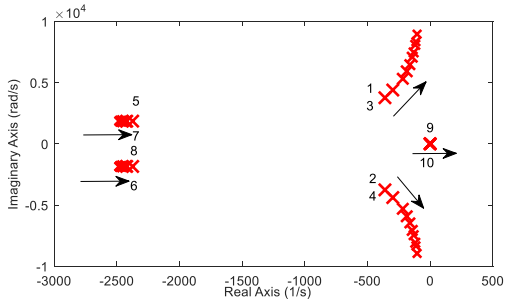

Figure 5 Impacts of the LC filter characteristics on the dynamic inverter model: $5mH \leq L_f \leq 25mH$ *and* $200\mu F \leq C_f \leq 40\mu F$

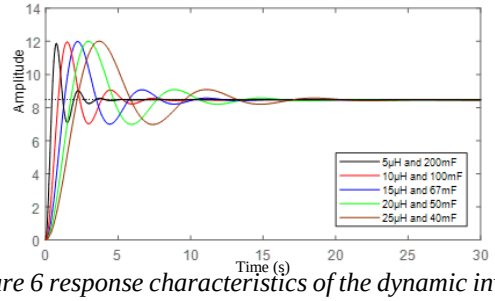

Figure 6 response characteristics of the dynamic inverter model: $5mH \leq L_f \leq 25mH$ *and* $200\mu F \leq C_f \leq 40\mu F$

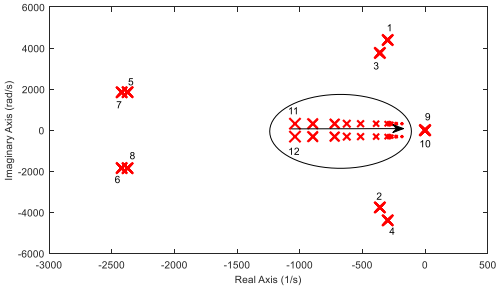

Figure 7 Impacts of the R/X *ration variation on the dynamic microgrid model:* $5{,}965 \leq \frac{R}{X} \leq 0.529$

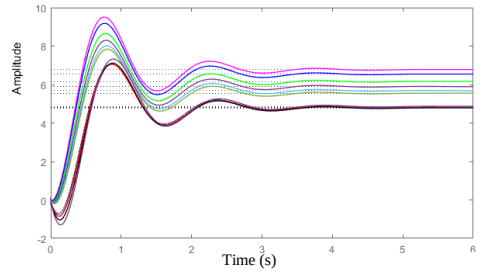

Figure 8 response characteristics of the dynamic microgrid model: $5{,}965 \leq \frac{R}{X} \leq 0.529$

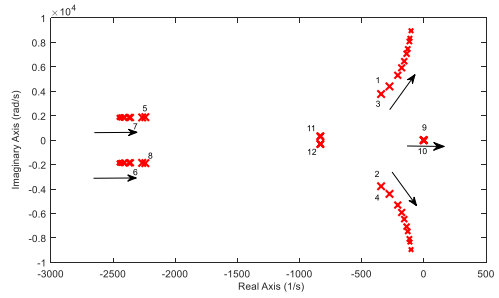

Figure 9 Impacts of the LC filter characteristics on the dynamic microgrid model: $5mH \leq L_f \leq 25mH$ *and* $200\mu F \leq C_f \leq 40\mu F$

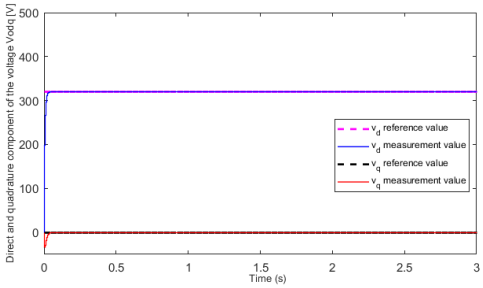

Figure 10 Control of the direct and quadrature components of the voltage at the output filter

CONCLUSION

The influence of filter characteristics and power distribution line parameters on the dynamical behaviour and performance of inverter-based islanded microgrids has been investigated through the microgrid small-signal model. This approach has been developed in the basic case of an islanded microgrid fed by a single inverter-based micro-source with constant impedance loads. The results obtained show that the inductor and capacitor of the filter more strongly affect the small-signal stability of the microgrid than the line parameters. The proposed approach has still to be tested in other architectures of islanded microgrids in order to establish its limits.

Acknowledgment
The authors would like to acknowledge the financial support provided by the CIA of UCL.

REFERENCES

[1] Z. Shuai, Y. Sun, Z. J. Shen, W. Tian, C. Tu, Y. Li, X. Yin, 2016, "Microgrid stability: Classification and a review", *Renewable and Sustainable Energy Reviews*, vol.58, 167–179.
[2] O. Palizban, K. Kauhaniemi, 2016, "Energy storage systems in modern grids-Matrix of technologies and applications", *Journal of Energy Storage*, vol.6, 248-259.
[3] G. Xiaozhi, L. Linchuan, C. Wenyan, 2011, "Power Quality Improvement for Mircrogrid in Islanded Mode", *Procedia Engineering*, vol. 23, 174 – 179.
[4] W Al-Saedi, S. W. Lachowicz, D. Habibi, O. Bass, 2013, "Voltage and frequency regulation based DG unit in an autonomous microgrid operation using Particle Swarm Optimization", *Electrical Power and Energy Systems*, vol. 53, 742–751.
[5] N. Pogak, M. Prodanovic, T. C. Green, 2007, "Modeling, Analysis and Testing of Autonomous Operation of an Inverter-Based Microgrid", *IEEE Transactions on Power Electronics*, vol. 22, 613-625.
[6] D. K. Dheer, N. Soni, S. Doolla, 2016, "Improvement of the small signal stability margin and transient response in inverter-dominated microgrids", *Susainable Energy, Grids and Networks*, vol.5, 135-147.